IJASRM International Journal of Advanced Scientific Research and Management, Special Issue 4, ICAMA-18, Apr 2019
www.ijasrm.com
ISSN 2455-6378

Green synthesis of zirconium, cerium & titanium doped cadmium oxide nanoparticles and its applications

V. Raja Rajeswari[1, 2], K.Lakshmi[2] and R.R. MuthuChudarkodi[3]*

[1] Research scholar, Reg. No. 17222232032010, PG & Research Department of Chemistry, V.O. Chidambaram College, Thoothukudi-628008, Tamilnadu, India

[2]Department of Chemistry, Sri Sarada College for women, Tirunelveli-62701, Tamilnadu, India

[3]PG & Research Department of Chemistry, V.O. Chidambaram College, Thoothukudi-628008, Tamilnadu, India.
(Affiliated to Manonmaniam Sundaranar University, Abishekapatti, Tirunelveli-627012, Tamilnadu, India)

Abstract

The present study concentrated on the environmentally friendly synthesizing of Cadmium Oxide nanoparticles (CdO NPs) and doped Cadmium Oxide nanoparticles with Zirconium (Zr), Cesium (Ce), and Titanium (Ti) using Acalypha indica extract of leaves and their potential applications. The field Emission Scanning electron microscopy (FESEM), X-ray diffraction spectroscopy (XRD), Fourier transform-infrared spectroscopy (FT-IR), UV Visible spectroscopy (UV-Vis), and Atomic Force microscopy (AFM) were used to characterize the produced tiny particles. The optical absorption has been determined and stated by UV Visible spectroscopy, with the range of wavelengths for the absorption peak 220, 236, 241, and 280 confirming the synthesis of CdO NPs, Ti-CdO NPs, Zr- CdO NPs, and Ce- CdO NPs, respectively. The typical size of the grains of CdO & doped NPs was 54.71 - 70.89 nm, and its crystal structure was determined employing XRD. FTIR verified the presence of CdO NPs and doped CdO in the band at the their respective where it is. FESEM was used to examine nano-sized materials; all synthesised products were nanometer in size. Its topography was deliberated by AFM analysis. As a result, this study reveals that CdO and doped nanoparticles are involved in a variety of applications.

Keywords: *CdO NPs, Acalypha Indica L, UV-Visible, SEM, FT-IR, XRD and AFM*

1. Introduction

Nanoparticles are employed in a wide range of uses, such as healthcare, electronic components, catalysts, and electricity. They are defined as elements with sizes that range from one nm to one hundred nm. The particles behave variously when compared to bulk counterparts at smaller size dimensions. When particles become lesser, their outermost area expands significantly. The development of nanotechnology as well as the utilization of new synthesised technological advances is a new and rapidly arising the field that utilizes for producing and preparing Nanomaterials may and thereby customizing use by alternately structures. As a result, the substance was created for the purpose of creating useful devices and systems by managing shape and size at the nanometer scale. This allows for the development of characteristics like increased electric and thermal resistance, decreased melting points, and enhanced magnetized and optical properties. The ability to frequently use content of this dimension in the development of novel substances opens up a world of possibilities in fields like clean energy, catalysis, and sensors, to name a few.

Recent advances demonstrate the importance of environmentally friendly green chemistry methods for the manufacture of metal oxide nanoparticles. Plants naturally contain manufacturing facilities for chemicals. They are easy to maintain as well as inexpensive. The plants contain biological molecules which have an excellent capacity for turning salts of metals to oxide of metal nanoparticles, which include carbohydrates, proteins, and coenzymes. Plants extracts of phytochemicals play a dual role in the nanoparticle creation manage, performing as either decreasing orstabilizing individuals.

Cadmium oxide (CdO) is a renowned II-VI n-type semiconductor with a cubic adopted (FCC) crystal form and a band gap that is direct of 2.2 eV due to

an abundance of interstitial fluid cadmium or vacancies of oxygen, that serve as twice imposed supporters. In the age of technology, multiple techniques for preparing CdO tiny particles have been employed, including solgel [7], solvothermal [8, micro emulsion method [9], precipitation method [10], and sonochemical method [11]. Among these techniques, the co-precipitation method is a simple methodology for producing homogeneous, pinhole-free thin films. On the other hand, the benefits include low cost, ease of manufacturing, and suitability for large area the deposition process. Furthermore, the absorbing behavior, shape, crystallization, groups with functions, and band gap of the composite materials were investigated via different methods such as XRD, SEM with EDAX, FT-IR, UV-Vis, photo catalytic activity, and antibacterial activity.

2. Materials and Methods

2.1. preparation of plant extract

Acalypha indica L. leaves are esteeming in Tamil Siddha medicine, it prospective to invigorate the body easily. It having alkaloids and hydrocyanic acid and peoples in India and Africa take it as food. The plant materials collected at Sri Sarada College campus in Tirunelveli, Tamil Nadu, and India. *Acalypha indica L*leaves were cleaned, chopped little pieces and washed with water/deionized water several times to eliminate impurities, powdered and kept in safe. 5.0gofpowderedofmaterials weighed using SHIMADZU - AUX 220 weighing balance until a constant weight was obtained, then taken in250mlconicalflaskcontaining 100mlofmillipure distilled water. The mixture was refluxed at 90 deg C for 20 Minutes, cooled at room temperature; the supernatant was filtered through whatman No.1. Volume of Plant extract prepared required volume for the synthesis reaction. The aqueous extract *Acalypha indica L* stored at 5 deg. C for the further reaction. All chemicals and reagents purchased from Sigma-Aldrich.

2.2. Measurements

CdO and doped CdO NPs were tested by XRD using a Gonio radius 240 with Cu (λ= 1.54060 Å) in the range of [10°–80 °]. FE-SEM examination using a high performance TESCAN MIRA3.The Atomic force microscopy analysis using the Nanosurf easy2scan BT02218 is profilometer – a sharp cantilever tip interacts with the sample surface sensing the local forces between the molecules of the tip and sample surface. UV–Vis spectral analysis was performed on a JASCO, V-600 Diffuse Reflectance spectrophotometer. FTIR measurements of samples prepared as KBr disks were performed on a Thermo Scientific Nicolet iS5 FTIR spectrometer.

2.3. Methods

100ml of *Acalyphaindica L*. aqueous extract, 3.0g Cadmium nitrateadded in 250 mL conical flask. The solution was uniformly distributed mixed for 60 minutes with a constant stirring at 400 rpm. The color changes observed. Then solution centrifuged the precipitate dried in a 250°C in an oven. After Dried powdered collected and examined the qualities as well as used for application studies. For doping, 3.0g Cadmium nitrate and 1.0 g Zirconylnitrate were taken and similar procedures as follows. [18]. Ceric sulphate, Potassium titanium oxalate chemicals used for Ce and Ti doping with CdO NPs.

3. Results and Discussion

3.1.UV-VIS spectra

The optical and absorbance properties of Cadmium Oxide NPs were investigated using UV-Visible diffuse reflectance spectrophotometer in the 200-900 nm wavelength range at the ambient temperature. As shown in the figure 1 absorption peak 220, 236, 241 and 280 which confirmed formation of CdO NPs, Ti-CdO NPs, Zr-CdO NPs, and Ce-CdO NPs respectively. The Ce, Zr and Ti doped in CdONPs, due to the varying of the optical properties. This result, absorption peaks swifts and valves changes which proves the doping. Metal doping with nanoparticles, provides the molecule's structure as UV and visible light absorption involves the promotion of electrons and orbitals from the ground state to higher states. The metal doped cadmium oxide nanoparticles exhibit strong blue emission, making them interesting for use in optical devices.

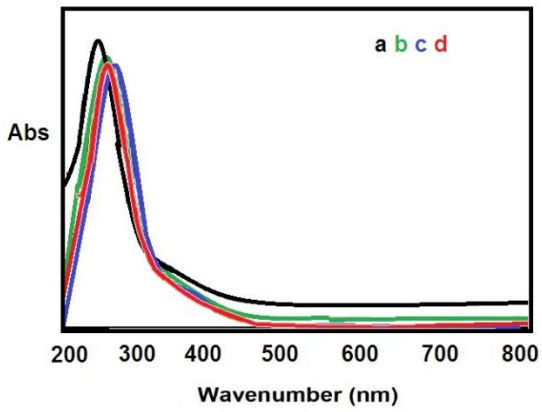

Figure 1 UV- Visible spectrum of a) CdO NPs, b) Zr- CdO NPs, c) Ce- CdO NPs and d) Ti- CdO NPs using *Acalypha indica* Leaf extract

3.2.XRD analysis

The crystallinity of CdO NPs and Zr/Ce/Ti doped CdO NPs was investigated using XRD with high intensity monochromatic radiation. Figure 2 depicts the XRD spectra of CdO NPs and Zr/Ce/Ti doped CdO NPs as a, b, c, and d.

$D = k\lambda / \beta\cos\theta$--------- (1)

Where D is the average crystalline size,

K is known as the Scherer's constant (K=0.94),

λ is the X-ray wavelength (1.54178Å),

β is full width at half maximum (FWHM) of the diffraction peak in degrees calculated values of nanoparticles was 54.71 –70.89 nm.

All of the diffraction patterns match well enough in terms of location and intensity sequence with the cubic crystal structure of pure CdO and doped as discovered in JCPDS Card No. 65-2908. The sharp and intense peaks indicate that the nanoparticles has been crystalline.The estimated size of the CdO NPs was found nano meter region, and sharp peaks show that particles were crystalline in nature. The peaks at the diffraction angles of 33.273, 38.591, 55.606, and 66.282° are indexed to the (111), (200), (220), and (311) planes, respectively. It is discovered that the as-prepared nanoparticles has a potent (11 1) preferential orientation. Usharani et al. [5] and Manjula et al. [6] obtained similar results.

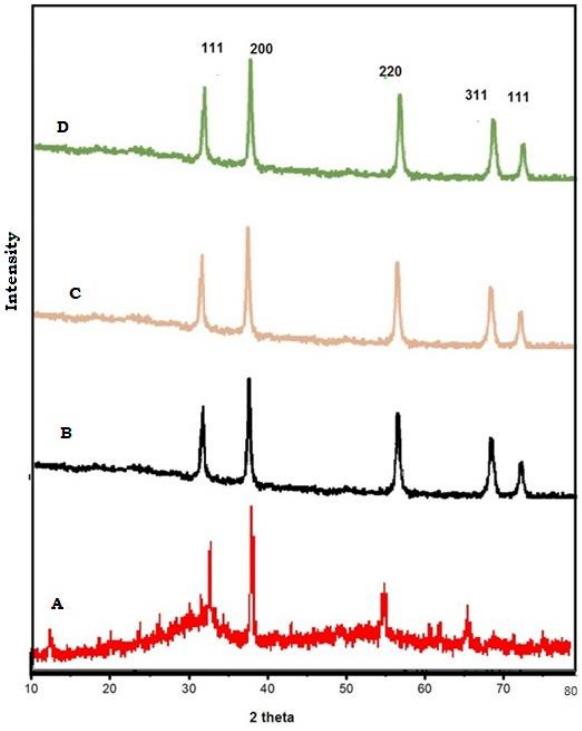

Figure 2 XRD of a) CdO NPs, b) Zr-CdO NPs, c) Ce-CdO NPs and d) Ti-CdO NPs using *Acalypha indica* Leaf extract

3.3. FTIR analysis

FTIR spectroscopy for functional groups analysis was recorded in the 400 to 1200 cm1 range. Figure 3 depicts this same FTIR spectrum of CdO NPs and Zr/Ce/Ti doped CdO NPs synthesised from *Acalypha indica* Leaf extract.

The metal-oxygen bond has been responsible for the broad bands seen at 714 and 613. Plant extracts with a higher concentration of phenolic and flavonoids, which are responsible for their antioxidant properties response, may play a part in the reduction, capping, and stabilization of NPs. The FTIR spectra also show that green synthesis procedures result in the bonding of hydroxyl group to the surface of NPs, as well as a variation in the intensity of each peak depending on the extract used.

The peaks at 1050 cm^{-1} and 795 cm^{-1} in figure 3 can be attributed to metal oxygen stretch of CdO NPs and also for doped NPs in figure 3 (a-d). Similarly, the observed peak at 545 cm^{-1} could be attributed to CdO stretching vibrations. The presence of CdO NPs is indicated by a band in the Cd-O at 881 cm^{1}. Figure 3 b) reveals that the stretching band vibrations for the Zr bond appear at 734 cm^{-1}, a significant band at 545 cm^{-1}, and a band at 466 cm-1 that is associated with Cd-O, confirming the emergence of Zr doped CdO NPs. Figure 3 c) Ce-CdO nanoparticles are created by detecting an important band at 473.05 and 551cm^{-1}. The IR spectrum of Ti-CdO NPs is depicted in Figure 3 d), and the strong band identified at 518 cm^{-1} to Cd-O stretching. The variations in peak positions clearly showed the existence of metabolic pathways such as polyphenolic compounds, flavones, naturally occurring substances, and terpenoids, which were abundant in the leaves extract and aided in the formation Process.

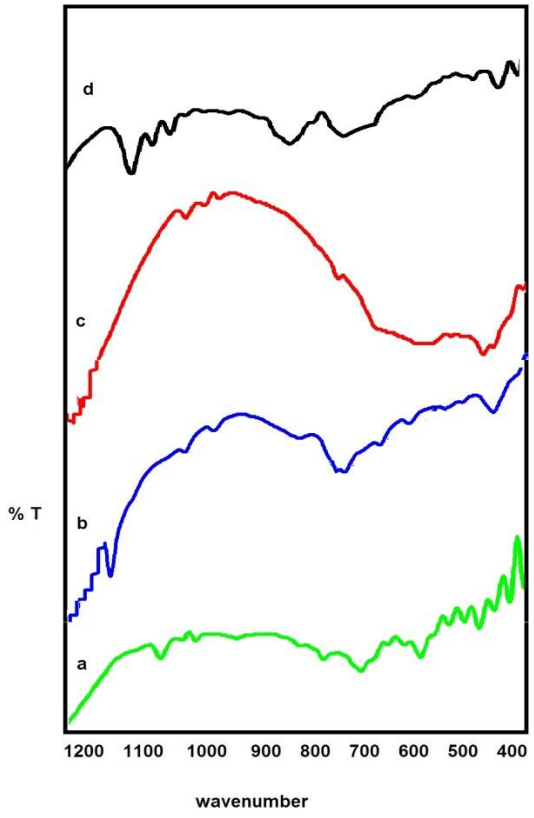

Figure 3 FTIR behavior of a) CdO NPs, b) Zr- CdO NPs, c) Ce-CdO NPs and d) Ti- CdO NPs using *Acalypha indica* Leaf extract

3.3. FESEM analysis

IJASRM International Journal of Advanced Scientific Research and Management, Special Issue 4, ICAMA-18, Apr 2019
www.ijasrm.com
ISSN 2455-6378

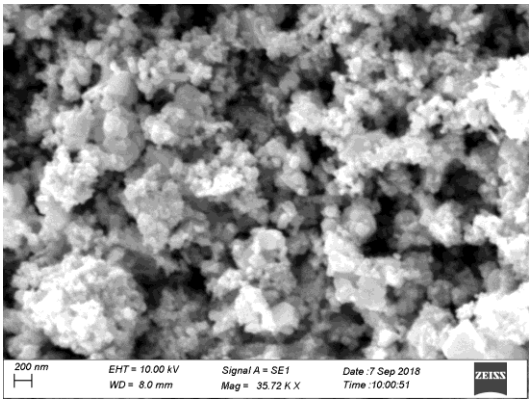

Figure 4 FESEM image of CdO NPs using *Acalypha indica* Leaf extract

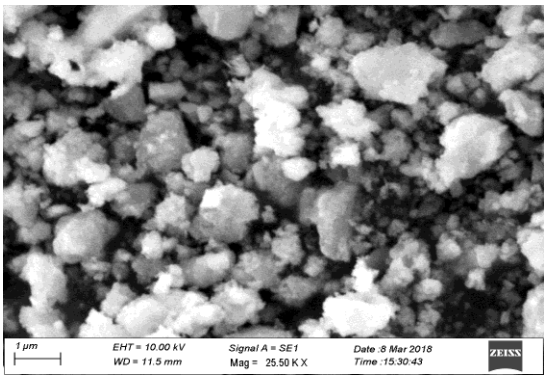

Figure 5 FESEM image of Zr-CdO NPs using *Acalypha indica* Leaf extract

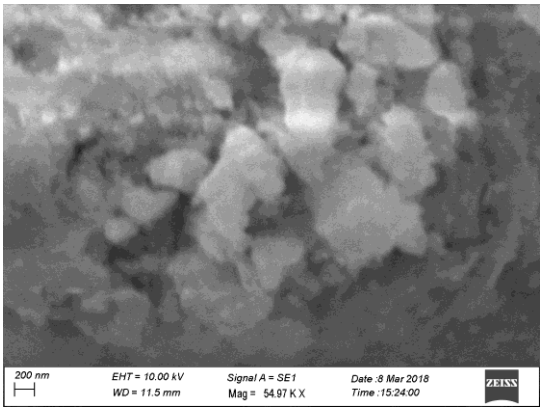

Figure 6 FESEM image of Ce-CdO NPs using *Acalypha indica* Leaf extract

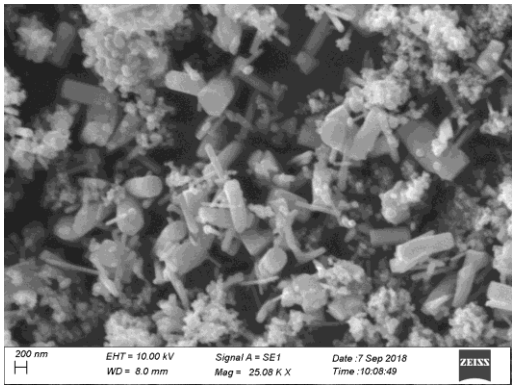

Figure 7 FESEM image of Ti-CdO NPs using *Acalypha indica* Leaf extract

Field emission scanning electron microscopy (FE-SEM) is a technique for identifying for image acquisition of the nanomaterials of a particle. FE-SEM images of CdO NPs and Zr/Ce/Ti doped CdO NPs are shown in Figures 4 - 7. Figure 4 illustrates FESEM images of Acalypha Indica leaf extract synthesised CdO-NPs with really tiny particles and spongy agreements, with ordinary particle sizes that vary from 33 to 50 nm. Figure 5 depicts Zr doped NiO NPs, with the metal doping expertly planned and the nanoparticle morphological characteristics of pebbles. The particles ranged in size from 40 to 100 nm. Figure 6 shows the perfect FESEM images of Ce-NiO NPs prepared from Acalypha Indica leaf extract. Ce- NiO NPs have a bacteria-like shape and an average size of 120 nm. Figure 7 depicts Ti-NiO NPs that are equal in both shape and size. The average size of the particles of Ti doped NPs ranges from 16.0 to 60 nm. This morphology appears to be rod surface. The diameter of nanoparticles was determined by the reflex speed as well as agitation time.

Table 1 Morphological behavior and particles sizes of Synthesized CdO NPs and Zr/Ce/Ti – doped CdO NPs.

S. No	Sources	Type of Morphology	Average Particle size
1.	CdO	Spongy	50.0
2.	Zr - CdO	Pebbles	100.0
3.	Ce - CdO	Bacterial	120.0
4	Ti - CdO	Rod	60.0

3.4. AFM analysis

Atomic force microscopy (AFM) is an effective means for visualising almost every texture, including polymeric materials, ceramic tiles, composite materials, crystal, and biological material. Many different forces, such as adhesion strength, magnetic forces, and mechanical properties, are measured and localised using AFM.Figures 8-11 depict the two-dimensional (2D) and three-dimensional (3D) surface texture of Cadmium oxide, Zr doped Cadmium oxide, Ce doped Cadmium oxide, and Ti doped Cadmium oxide nanoparticles, respectively. The Nanoscan 2 easy surf instrument was employed to investigate the manufactured Nanostructures.The image of Cadmium oxide Nanoparticles in Fig. 8 shows an even particle distribution and particles that are very small nearly 50 nm in size. The liner valley arrangement is depicted in 3D images. Figure 9 depicts Zr doped cobalt oxide nanoparticles, both 2 D and 3 D, demonstrating nanocomposites blending from the highest and valley morphologies and 120 nm in size. Figure 10 displayed planner topography as well as FESEM images that were overlaid such as structures of Ce doped Cadmium

IJASRM
International Journal of Advanced Scientific Research and Management, Special Issue 4, ICAMA-18, Apr 2019
www.ijasrm.com
ISSN 2455-6378

oxide nanoparticles, and Figure 11 reveals Ti doped Cadmium oxide nanoparticles and average particle size are near 100 nm and its 3 D image made clear that the combining of metallic materials and molecules occurs only at the nanometer scale zone.

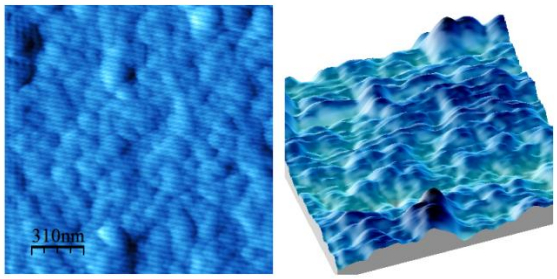

Figure 8.AFM images of Cadmium oxide NPs using *Acalypha indica L* leaf extract.

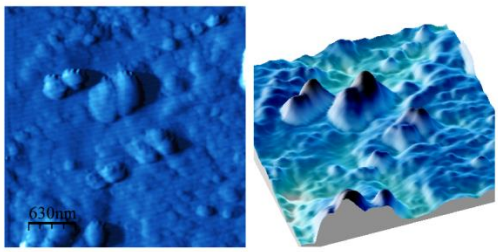

Figure 9AFM images of Zr doped Cadmium oxide NPs using *Acalypha indica L* leaf extract.

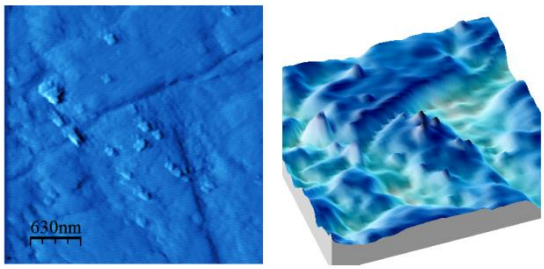

Figure 10.AFM images of Ce doped Cadmium oxide NPs using *Acalypha indica L* leaf extract.

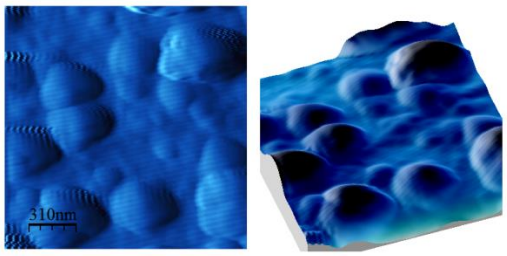

Figure 11AFM images of Ti doped Cadmium oxide NPs using *Acalypha indica L* leaf extract.

3.5. Anti-microbial activity

Agar well diffusion is a common method for determining the antibacterial activities of plant or microbial extracts. The diffusion on agar wells method was used to explore the anti-bacterial behavioural patterns of CdO NPs and Zr/Ce/Ti doped CdO NPs. Antimicrobial activity has the possibility of predicting treatment efficacy, as well as aid in developing drugs and epidemiological studies. With us primary objective is to use antimicrobial test methods to evaluate concentrates and pure medicines as potential antibacterial agents in vitro. Agar disk-diffusion testing, first attempted in 1940, appears to be the accepted method for routine bacteriological examination in so many microbiology laboratory labs.

Our nanomaterials were evaluated in a therapeutic applications research lab against the pathogen Aspergillus fumigates. A 24-hour culture of the bacterial strain Aspergillus fumigates was implanted into petri plates containing 20ml agar media. Wells were cut and various concentrations of sample CdO NPs and Zr/Ce/Ti doped CdO NPs (500 g/ml, 250 g/ml, 100 g/ml, and 50 g/ml) were presented. The plates were then incubated for 24 hours at 37°C. The diameter of the inhibitory zone formed around the wells was measured to assess anti-bacterial activity. As a positive control, amphoteric in B was used. The values were computed using the Graph Pad Prism 6.0 software (USA). Results of anti-bacterial study shown in Fig.4.21 a) CdO NPs (1), b) Zr- CdO NPs (2), c) Ce- CdO NPs (3) and d) Ti- CdO NPs (4).

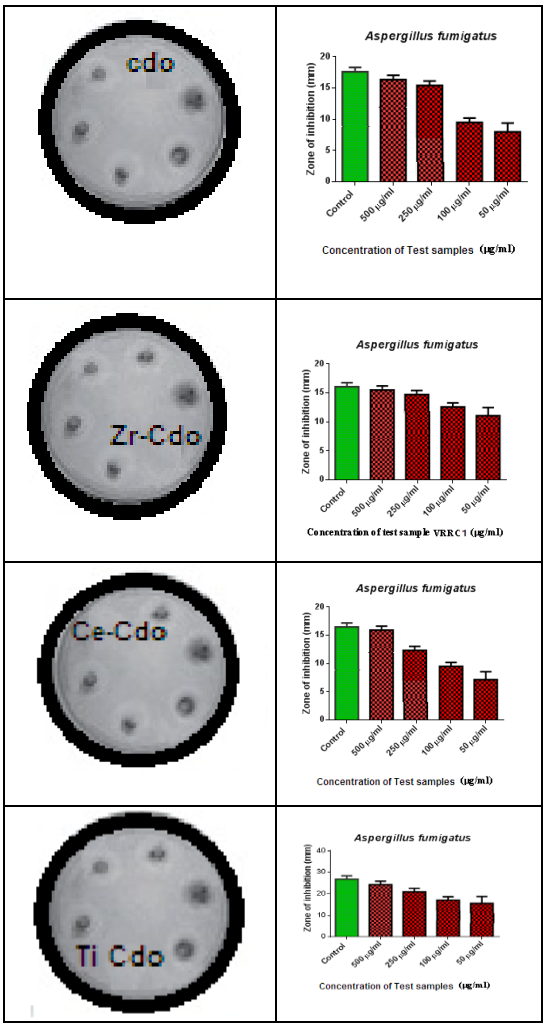

Figure 12 the antimicrobial activity of CdO NPs & Zr/Ce/Ti doped CdO NPs *against the pathogens Aspergillus fumigates*

Table 2Mean ±SD of zone of inhibition obtained by sample CdO NPs and Zr/Ce/Ti doped CdO NPs *Aspergillus fumigatus*

nanomaterials	Zone of inhibition (mm) Mean ± SD				
	500 µg/ml	250 µg/ml	100 µg/ml	50 µg/ml	Control (Ab)
CdO	16.9 ±1.0	16.0 ±0.5	11.8 ±1.0	10.1 ±0.5	18.0 ±0.5
Zr-CdO	17.1 ±0.5	16.5 ±0.5	15.8 ±0.5	12.5 ±0.5	16.5 ±0.5
Ce- CdO	16.7 ±0.5	15.5 ±0.5	11.6 ±0.5	8.5 ±0.5	15.5 ±0.5
Ti- CdO	26.3 ±1.0	20.5 ±0.5	19.2 ±0.5	18.5 ±1.5	28.0 ±0.5

According to the results of Figure 12 and Table 2 raising the concentration of CdO NPs and Zr/Ce/Ti doped Cadmium oxide NPs is associated with expanding the zones of inhibition even against pathogen Aspergillus fumigatus. Ti doped Cadmium oxide NPs have the strongest antimicrobial properties of every Nano particle that has been produced.

3.6 Photo catalytic analysis

Nanosized CdO and Zr/Ce/Ti doped CdO NPs are effective photocatalysts for the degradation of organic contaminants such as crystal violet dye. To make the dye solution, dissolve 10mg powder crystal violet dye in 100ml distilled water. 0.1g CdO and Zr/Ce/Ti doped CdO NPs were added to 100ml of prepared crystal violet dye solution and magnetically stirred for 1 hour in the shadow before being exposed to sunlight. The colloidal suspension was then placed in a closed chamber and exposed to sunlight. For 1 hour, the reactions were observed one by one at 10-minute intervals. Finally, the rate of dye decomposition was measured by collecting samples from each set and recording the UV-Vis spectra in the wavelength after centrifugation and filtration.

At 590 nm, the UV visible absorbance values of pure crystal violet dye solution are visible. The characteristic absorbance value at 590 nm was used to monitor the photocatalytic degradation process. Figures show that there were no significant changes in the concentration of Crystal violet dye after 1 hour of irradiation, indicating that pure Crystal violet dye solution cannot be easily degraded by UV light. The degradation efficiency of pure crystal violet dye after 1 hour of irradiation was approximately 71%, as shown in Table.3.

The degradation of crystal violet dye in the existence of bio synthesized CdO nanoparticles has been demonstrated by that of the lowering in absorption peak during one 60-minute exposed to solar light, as shown in Fig.13-16. The dye degradation (%) was calculated using the following equation (2), and its variation with exposure period is shown in Fig.13-16.

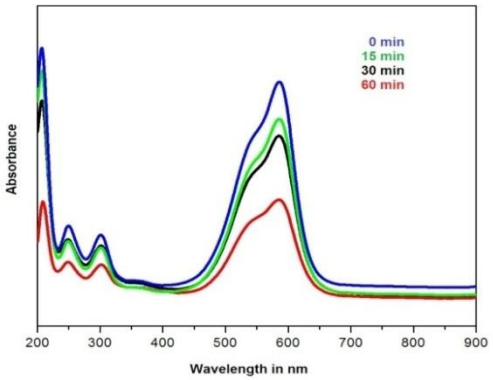

Fig.13. UV-Visible absorption spectra of Crystal violet dye in the presence of CdO NPs synthesized using *Acalypha indica* leaf extract

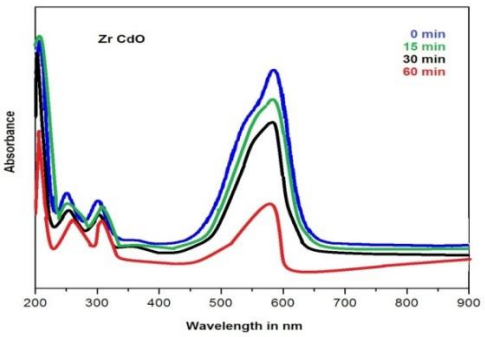

Fig.14 UV-Visible absorption spectra of Crystal violetdye in the presence of Zr-CdO NPs synthesized using *Acalypha indica* leaf extract

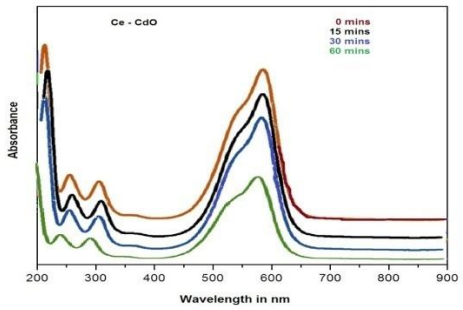

Fig.15 UV-Visible absorption spectra of Crystal violet dye in the presence of Ce-CdO NPs synthesized using *Acalypha indica* leaf extract

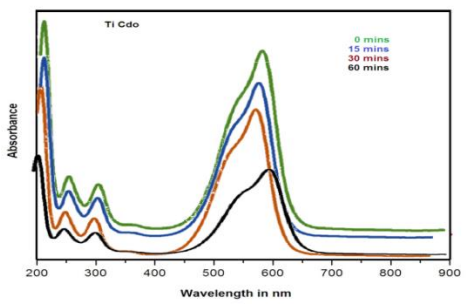

Fig. 16 UV-Visible absorption spectra of Crystal violet dye in the presence of Ti-CdO NPs synthesized using *Acalypha indica* leaf extract

$$Efficiency = \left[1 - \frac{C}{C0}\right] x100\text{-----} \quad (2)$$

Where C0 is the initial concentration of crystal violet and C is the dye solution concentration at the chosen irradiation time. The absorbance spectra revealed that the maximum degradation efficiency of crystal violet dye occurred within 60 minutes of irradiation. The results showed that CdO improves degradation efficiency. As a result, CdO nanoparticles have significantly higher photocatalytic activity. The effectiveness of degradation of dyes was determined by calculating using equation no.2, and the results are summarised in table 3.

Table.3. Comparison of Degradation efficiency of CdO NPs, Zr/Ce/Ti doped CdO NPs synthesized using *Acalyphaindica* leaf extract

Time (min)	Efficiency (%)			
	CdO	Zr- CdO	Ce-CdO	Ti-CdO
0	-	-	-	-
10	41	46	40	57
30	50	51	52	65
60	62	57	59	74

Table. 3 compares the degradation efficiency of CdO NPs and Zr/Ce/Ti doped CdO NPs synthesised from *Acalyphaindica* leaf extract. According to the absorbance spectra, the maximum degradation efficiency of crystal violet dye within 60 minutes of irradiation time was approximately 62% for CdO NPs, 57% for Zr-NiO NPs, 59% for Ce-NiO NPs, and 74% for Ti-CdO NPs. The findings revealed that synthesised nanomaterials improve degradation efficiency. As a result, the produced nanoparticles have much greater photo catalytic capacity than pure dye.

5. Conclusions

CdO NPs and Zr/Ce/Ti doped CdO NPs were successfully synthesised using *Acalypha indica L*eaf extract in a concise green approach. In the UV–visible spectrum, a prominent peak at 220 to 280 nm was found, which confirming the formation of synthesised nanoparticles. According to Debye–formula, Scherrer's CdO NPs with an average crystallographic size of 54 to 70 nm and have a cubic structure as determined XRD patterns, it well associated with JCPDS files. The FESEM studies confirms the formation CdO NPs and doped NPs is in the nano meter range (50 nm to 120 nm). The FT-IR spectra of CdO NPs and doped NPs revealed a prominent band at 714 $cm^{-1}$and 613 cm^{-1} that corresponded to the vibration of the Cd-O bond. The antibacterial activity of CdO NPs and doped NPs shown excellent inhibitory action against water-borne diseases. The produced nanocrystalline materials in this work proved promising for prospective medicinal applications due to its competent antifungal and antibacterial capabilities. Cadmium oxide (CdO) and its doped materials have been investigated for their photo catalytic behavior in an array of fields such as polluting substances degradation.

Acknowledgments

The authors are grateful to the Department of Science and Technology (FAST TRACK and FIST) in New Delhi, India for using the CHI Electro Chemical workstation and Jasco UV-VISIBLE Spectrophotometer at V.O. Chidambaram College, Thoothukudi-8

Reference

1. Virendra K Sharma, Ria A Yngard and Yekaterina Lin Advances in colloids and interface science, 2009, volume 145 issue 1-2 page no 83-96.
2. Khadeejparveen, Victoria Banse and lalitaLedwani Green synthesis of nanoparticles their advantages and disadvantages AIP conference proceedings, 2016, 1724, 020048.
3. Karpagavinayagam P, Vedhi C, Green synthesis of iron oxide nanoparticles using Avicennia marina flower extract, Vacuum, 160(2019) 286-292.
4. Battin T.J., von der Kammer F., Weilhartner A., Ottofuelling S., Hofmann T. Nanostructured TiO_2: Transport Behavior and Effects on Aquatic Microbial Communities under Environmental Conditions. *Environ. Sci. Technol.* 43(2009)8098–8104.
5. Noh, Y.W., Lee, J.H., Jin, I.S., Park, S.H. and Jung, J.W., 2019. Tailored electronic properties of Zr-doped SnO2 nanoparticles for efficient planar perovskite solar cells with marginal hysteresis. Nano Energy, 65, p.104014.
6. Blum, J. L., Xiong, J. Q., Hoffman, C., & Zelikoff, J. T. (2012). Cadmium associated with inhaled cadmium oxide nanoparticles impacts fetal and neonatal development and growth. Toxicological Sciences, 126(2), 478-486.
7. Kumar A., Jena P.K., Behera S., Lockey R.F., Mohapatra S., Mohapatra S. Multifunctional magnetic nanoparticles for targeted delivery. *Nanomed. Nanotechnol. Biol. Med.* 6(2010)64–69..
8. Kaviyarasu K., Geetha N., Kanimozhi K., Magdalane C.M., Sivaranjani S., Ayeshamariam A., Kennedy J., Maaza M. In vitro cytotoxicity effect and antibacterial performance of human lung epithelial cells A549 activity of Zinc oxide doped TiO 2 nanocrystals: Investigation of bio-medical application by chemical method. *Mater. Sci. Eng. C.* 74(2017)325–333.
9. Gowri S., Gopinath K., Arumugam A. Experimental and computational assessment of mycosynthesized CdO nanoparticles towards biomedical applications. *J. Photochem. Photobiol. B Biol.* 180(2018)166–174..
10. K. Chen, S. K. Yuan, P. L. Li, F. Gao, J. Liu, G. L. Li, A. G. Zhao, X. M. Lu, J. M. Liu, and J. S. Zhu, High permittivity in Zr doped NiO ceramics, API Journal of Applied physics, 2007.
11. Mishra P.K., Mishra H., Ekielski A., Talegaonkar S., Vaidya B. Zinc oxide nanoparticles: A promising nanomaterial for biomedical applications. *Drug Discov. Today.* 22(2017)1825–1834.

12. Mostafa, A. M., Yousef, S. A., Eisa, W. H., Ewaida, M. A., & Al-Ashkar, E. A. (2017). Synthesis of cadmium oxide nanoparticles by pulsed laser ablation in liquid environment. Optik, 144, 679-684.
13. Khorsand Zak A., Razali R., Abd Majid W.H., Darroudi M. Synthesis and characterization of a narrow size distribution of zinc oxide nanoparticles. *Int. J. Nanomed.* 6(2011)1399.
14. Li, J., Li, P., Li, J., Tian, Z. and Yu, F., 2019. Highly-dispersed Ni-NiO nanoparticles anchored on an SiO_2 support for an enhanced CO methanation performance. Catalysts, 9(6), p.506.
15. Leandro Andrini,a Paula C. Angelomé, Galo J. A. A. Soler-Illiac,d and Félix G. Requejoa, Understanding the Zr and Si interdispersion in Zr1−xSixO2 mesoporous thin films by using FTIR and XANES spectroscopy, Dalton Transactions (RSC) 2016.
16. P. Karpagavinayagam and C. Vedhi. Green synthesis of novel nickel oxide nanoparticles using mangroves and its electrochemical characterization, International Journal of Science, Engineering and Management, 2018,
17. Saha, B., Das, S., & Chattopadhyay, K. K. (2007). Electrical and optical properties of Al doped cadmium oxide thin films deposited by radio frequency magnetron sputtering. Solar energy materials and solar cells, 91(18), 1692-1697.
18. Natu, G., Hasin, P., Huang, Z., Ji, Z., He, M. and Wu, Y., 2012. Valence band-edge engineering of nickel oxide nanoparticles via cobalt doping for application in p-type dye-sensitized solar cells. ACS applied materials & interfaces, 4(11), pp.5922-5929.
19. Sharma R.K., Ghose R. Synthesis of zinc oxide nanoparticles by homogeneous precipitation method and its application in antifungal activity against Candida albicans. *Ceram. Int.* 41(2015)967–975.
20. Ajay Savale, Suresh Ghotekar, ShreyasPansambal and OnkarPardeshi, Green Synthesis of Fluorescent CdO Nanoparticles using Leucaenaleucocephala L. Extract and their Biological Activities, J Bacteriol Mycol Open Access, 5(5): 00148, 2017.
21. Wang Y., Zhang C., Bi S., Luo G. Preparation of ZnO nanoparticles using the direct precipitation method in a membrane dispersion micro-structured reactor. *Powder Technol.* 202(2010)130–136.
22. Jung Kyu Kim, PEG-assisted Sol-gel Synthesis of Compact Nickel Oxide Hole-Selective Layer with Modified Interfacial Properties for Organic Solar Cells,Polymers 2019, 11, 120; doi:10.3390/polym11010120
23. Saeid Taghavi Fardood, Ali Ramazani, Sajjad Moradi ,A novel green synthesis of Nickel oxide nanoparticles using arabic gum, Chemistry journal of Moldova. General, Industrial and Ecological Chemistry, 2017, 12(1), 115-118.
24. Ramakrishnan Azhagu Raj, Mohamad S. Al Salhi, and Sandhanasamy Devanesan Microwave- Assisted Synthesis of Nickel Oxide Nanoparticles Using Coriandrum sativum Leaf Extract and Their Structural-Magnetic Catalytic Properties Materials 2017, 10, 460.
25. CLSI, Performance Standards for Antimicrobial Disk Susceptibility Tests, Approved Standard, 7th ed., CLSI document M02-A11. Clinical and Laboratory Standards Institute, 950 West Valley Road, Suite 2500, Wayne, Pennsylvania 19087, USA, 2012.
26. CLSI, Method for Antifungal Disk Diffusion Susceptibility Testing of Yeasts, Approved Guideline. CLSI document M44-A. CLSI, 940 West Valley Road, Suite 1400, Wayne, Pennsylvania 19087-1898, USA, 2004.
27. Buraso W., Lachom V., Siriya P., Laokul P. Synthesis of TiO_2 nanoparticles via a simple precipitation method and photocatalytic performance. *Mater. Res. Express.* 5(2018)115003.
28. Fu G., Vary P.S., Lin C.-T. Anatase TiO 2 Nanocomposites for Antimicrobial Coatings. *J. Phys. Chem. B.* 109(2005)8889–8898.
29. DurgaVijaykarthik, D., Kirithika, M., Prithivikumaran, N., & Jeyakumaran, N. (2014). Synthesis and characterization of Cadmium Oxide nanoparticles for antimicrobial activity.
30. Hu C., Lan Y., Qu J., Hu X., Wang A. $Ag/AgBr/TiO_2$ Visible Light Photocatalyst for Destruction of Azodyes and Bacteria. *J. Phys. Chem. B.* 110(2006)4066–4072.
31. Kumar, S., Ojha, A. K., & Walkenfort, B. (2016). Cadmium oxide nanoparticles grown in situ on reduced graphene oxide for enhanced photocatalytic degradation of methylene blue dye under ultraviolet irradiation. Journal of Photochemistry and Photobiology B: Biology, 159, 111-119.
32. Senobari, S., & Nezamzadeh-Ejhieh, A. (2018). A comprehensive study on the photocatalytic activity of coupled copper oxide-cadmium sulfide nanoparticles. Spectrochimica Acta Part A: Molecular and Biomolecular Spectroscopy, 196, 334-343.
33. Jana, T. K., Maji, S. K., Pal, A., Maiti, R. P., Dolai, T. K., & Chatterjee, K. (2016). Photocatalytic and antibacterial activity of cadmium sulphide/zinc oxide nanocomposite with varied morphology. Journal of colloid and interface science, 480, 9-16